

# Characterizing Universal Gate Sets via Dihedral Benchmarking

Arnaud Carignan-Dugas,<sup>1</sup> Joel Wallman,<sup>1</sup> and Joseph Emerson<sup>1,2</sup>

<sup>1</sup>*Institute for Quantum Computing and the Department of Applied Mathematics,  
University of Waterloo, Waterloo, Ontario N2L 3G1, Canada*

<sup>2</sup>*Canadian Institute for Advanced Research, Toronto, Ontario M5G 1Z8, Canada*

(Dated: July 26, 2018)

We describe a practical experimental protocol for robustly characterizing the error rates of non-Clifford gates associated with dihedral groups, including gates in  $SU(2)$  associated with arbitrarily small angle rotations. Our dihedral benchmarking protocol is a generalization of randomized benchmarking that relaxes the usual unitary 2-design condition. Combining this protocol with existing randomized benchmarking schemes enables an efficient means of characterizing universal gate sets for quantum information processing in a way that is independent of state-preparation and measurement errors. In particular, our protocol enables direct benchmarking of the  $T$  gate (sometimes called  $\pi/8$ -gate) even for the gate-dependent error model that is expected in leading approaches to fault-tolerant quantum computation.

A universal quantum computer is a device allowing for the implementation of arbitrary unitary transformations. As with any scenario involving control, a practical quantum computation will inevitably have errors. While the complexity of quantum dynamics is what enables the unique capabilities of quantum computation, including important applications such as quantum simulation and Shor’s factoring algorithm, that same complexity poses a unique challenge to efficiently characterizing the errors. One approach is quantum process tomography [1, 2], which yields an informationally-complete characterization of the errors on arbitrary quantum gates, but requires resources that scale exponentially in the number of qubits. Moreover, quantum process tomography can not distinguish errors associated with the quantum gates from those associated with state-preparation and measurement (SPAM) [3].

Randomized benchmarking [4–7] using a unitary 2-design [8, 9], such as the Clifford group, overcomes both of these limitations by providing an estimate of the error rate per gate averaged over the 2-design. More specifically, it is a method for efficiently estimating the average fidelity

$$\mathcal{F}_{\text{avg.}}(\mathcal{E}) := \int d\psi \langle \psi | \mathcal{E}(\psi) | \psi \rangle \quad (1)$$

of a noise map  $\mathcal{E}$  associated with any group of quantum operations forming a unitary 2-design in a way that is independent of SPAM errors. This partial information is useful in practice as it provides an efficient means of tuning-up experimental performance, and, moreover, provides a bound on the threshold error rate required for fault tolerant quantum computing [10], a bound that becomes tight when the noise is stochastic [7, 11].

An important limitation of existing randomized benchmarking methods is that they are only efficient in the number of qubits [4, 6, 9] for non-universal sets of gates such as the Clifford group. While Clifford gates play an important role in leading approaches to fault-tolerant quantum computation based on stabilizer codes [10], one

still needs a means of benchmarking the remaining non-Clifford gates required for universality; this is particularly important because the non-Clifford gates will be implemented via magic state distillation and gate injection [12, 13], which is a complex procedure that will be subject to dramatically different error rates than those of the (physical or logical) Clifford gates.

In the present paper, we describe a protocol for benchmarking the average fidelity of a group of operations corresponding to the dihedral group which does not satisfy the usual 2-design constraint for randomized benchmarking. However, we show that the dihedral benchmarking protocol still allows the average fidelity to be estimated while retaining the benefits of standard randomized benchmarking. Furthermore, by combining our dihedral benchmarking protocol with both standard [6] and interleaved randomized benchmarking [14], we give an explicit method for characterizing the average fidelity of the  $T$  gate directly. This is of particular interest because the  $T$  gate combined with the generators of the Clifford group (e.g., the CNOT, the Hadamard and the Pauli gates) provides a standard gate set for generating universal quantum computation. Moreover our protocol enables characterization of non-Clifford gates associated with arbitrarily small angle rotations, which are of interest to achieve more efficient fault-tolerant circuits [15–17]. Remarkably, our protocol overcomes the key assumption of ‘weak gate-dependence’ of the noise that limits previous benchmarking protocols. Specifically, the protocol is robust in the important setting when the error on the non-Clifford gate, such as the  $T$  gate, is substantially different from the error on the Clifford operations. As noted above, this is the expected scenario in leading approaches to fault-tolerant quantum computation.

*Characterizing single-qubit unitary groups.*—We now outline a protocol that yields the average gate fidelity of the experimental implementation of a single-qubit unitary group of the form

$$\mathcal{D}_j = \langle R_j(1), X \rangle, \quad (2)$$

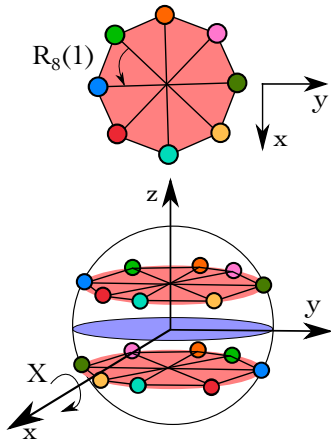


FIG. 1. The orbit, under the action of the dihedral group  $\mathcal{D}_8$ , of an input state located at a  $45^\circ$  degree latitude on the Bloch sphere.  $R_8(z)$  are the rotations of the octagon, while  $X$  is a reflection (or a rotation in 3 dimensions, with the rotation axis parallel to the octagon's surface). The  $T$  gate corresponds to the smallest rotation  $R_8(1)$ .

where  $j$  is a positive integer and

$$R_j(z) := e^{2\pi izZ/j} = \cos(2\pi z/j)\mathbb{I} + i \sin(2\pi z/j)Z. \quad (3)$$

Up to an overall sign,  $\mathcal{D}_j$  is a representation of the dihedral group of order  $2j$ , with  $XR_j(z) = R_j(z+j)X$ , which is not a unitary 2-design and includes gates producing arbitrarily small rotations as  $j$  increases. Note that the choice of rotation axis is arbitrary, and that any single-qubit gate can be written as  $R_j(1)$  relative to some axis. Consequently, our protocol will allow any single-qubit gate to be benchmarked. The Bloch sphere representation of  $\mathcal{D}_8$  acting on a qubit state is illustrated in fig. 1. This group contains the so-called  $T$  gate, which corresponds to the  $R_8(1)$  rotation.

The dihedral benchmarking protocol is as follows.

1. Choose two binary strings of length  $m$ ,  $\mathbf{z} = (z_1, \dots, z_m) \in \mathbb{Z}_2^m$  and  $\mathbf{x} = (x_1, \dots, x_m) \in \mathbb{Z}_2^m$  independently and uniformly at random.
2. Prepare a system in an arbitrary initial state  $\rho$ .<sup>1</sup>
3. At each time step  $t = 1, \dots, m$ , apply  $R_j(z_t)X^{x_t}$ .
4. Apply the inversion gate, defined as

$$G_{\text{inv.}} := X^{b_1}Z^{b_2} \prod_{t=1}^m [R_j(z_t)X^{x_t}]^\dagger,$$

where  $b_1, b_2 \in \mathbb{Z}_2$  are fixed by considerations below.

5. Perform a POVM  $\{E, \mathbb{I} - E\} \rightarrow \{+1, -1\}$  for some  $E \approx \rho$ , to estimate the probability  $q(+1|m, x, z, b_1, b_2)$  of outcome  $+1$ .

6. Repeat steps 1-5  $k$  times, where  $k$  is fixed by the requirement to estimate the survival probability

$$\Pr(m, b_1, b_2) := |2j|^{-(m+1)} \sum_{x,z} q(+1|m, x, z, b_1, b_2)$$

to a desired precision (see [7, 18, 19] for details on the required sampling complexity).

For  $b_1 = b_2 = 0$ , the average survival probability is

$$\Pr(m, 0, 0) = Ap_0^m + Bp_1^m + C, \quad (4)$$

where  $A, B$  and  $C$  are constants absorbing SPAM factors. Because a sum of two exponentials leads to a non-linear fitting problem, it should generally be advantageous to fit instead to

$$\begin{aligned} &\Pr(m, 0, 0) + \Pr(m, 0, 1) \\ &- \Pr(m, 1, 0) - \Pr(m, 1, 1) = 4Ap_0^m \end{aligned} \quad (5)$$

and

$$\Pr(m, 0, 0) - \Pr(m, 0, 1) = 2Bp_1^m. \quad (6)$$

As we will show below, the average gate fidelity is related to the fit parameters  $p_0$  and  $p_1$  by

$$\mathcal{F}_{\text{avg.}}(\mathcal{E}) = \frac{1}{2} + \frac{1}{6}(p_0 + 2p_1). \quad (7)$$

*Analysis.*—We now derive the formula for the decay curves expressed in eqns. 4–6, together with the average fidelity eqn. 7. We assume that the experimental noise is completely positive and trace-preserving and is also gate and time-independent (though perturbative approaches to relax these assumptions can be considered [7, 19]), so that we can represent the experimental implementation of  $\mathcal{R}_j(z) \circ \mathcal{X}^x$  as  $\mathcal{E} \circ \mathcal{R}_j(z) \circ \mathcal{X}^x$ . We use calligraphic font to denote abstract channels (where, for a unitary  $U$ , the abstract channel  $\mathcal{U}$  corresponds to conjugation by  $U$ ) and  $\circ$  to denote channel composition (i.e.,  $\mathcal{B} \circ \mathcal{A}$  means apply  $\mathcal{A}$  then  $\mathcal{B}$ ). We refer to

$$\mathcal{E}^{\mathcal{G}} = (|\mathcal{G}|)^{-1} \sum_{U \in \mathcal{G}} U^{-1} \circ \mathcal{E} \circ U \quad (8)$$

as the *twirl* of  $\mathcal{E}$  over a group  $\mathcal{G}$ . Averaged over all sequences  $x$  and  $z$  of length  $m$ , our protocol yields the following effective channel

$$\mathcal{C} = \mathcal{E} \circ \mathcal{X}^{b_1}Z^{b_2} \circ (\mathcal{E}^{\mathcal{D}_j})^{\circ m}. \quad (9)$$

The Pauli-Liouville representation (see, e.g., Ref. [19] for details) of an abstract channel  $\mathcal{E}$  consists in a matrix of inner products between Pauli matrices  $P_j$  and their images  $\mathcal{E}(P_k)$

$$\mathcal{E}_{jk} = \text{Tr}(P_j \mathcal{E}(P_k)). \quad (10)$$

<sup>1</sup> The constants  $A$  and  $B$  appearing in eqns. 5 and 6 depend on state preparation, as shown in eqns. 15–17. These constants may be maximized by choosing an appropriate state preparation (and the corresponding measurement). In particular, optimal states for eqn. 5 and eqn. 6 are  $|0\rangle\langle 0|$  and  $|+\rangle\langle +|$  respectively.

We denote this representation with the bold font  $\mathcal{E}$ . The Pauli-Liouville representation of  $\mathcal{D}_j$  is a direct sum of three inequivalent irreducible representations (irreps) of the dihedral group:

1.  $R_j(z)X^x \rightarrow 1$  (trivial representation)
2.  $R_j(z)X^x \rightarrow \begin{pmatrix} \cos(2\pi z/j) & (-1)^{x+1} \sin(2\pi z/j) \\ \sin(2\pi z/j) & (-1)^x \cos(2\pi z/j) \end{pmatrix}$  (faithful representation)
3.  $R_j(z)X^x \rightarrow (-1)^x$  (parity representation).

This is easily seen by looking at the action of  $\mathcal{D}_j$  on the Bloch sphere (see fig. 1). The trivial representation emerges from the unitality and trace-preserving properties of unitary operations, which map any Bloch shell of constant radius to itself, including the center point. The parity representation encodes the fact that the  $\pm Z$  poles of the Bloch sphere are invariant under conjugation by  $R_j(z)$  and swapped under conjugation by  $X$ . The two-dimensional representation encodes the action of  $R_j(z)X^x$  on the  $XY$ -plane of the Bloch sphere.

As a consequence of Schur's lemmas (see the supplementary information of Ref. [20]), the twirled noise channel is a direct sum of three identity matrices:

$$\mathcal{E}^{\mathcal{D}_j} = \begin{pmatrix} 1 & 0 & 0 & 0 \\ 0 & p_1 & 0 & 0 \\ 0 & 0 & p_1 & 0 \\ 0 & 0 & 0 & p_0 \end{pmatrix}, \quad (11)$$

where  $p_0 := \mathcal{E}_{44}$  and  $p_1 := \frac{\mathcal{E}_{22} + \mathcal{E}_{33}}{2}$ . With these definitions, the average fidelity is [21, 22]

$$\begin{aligned} \mathcal{F}_{\text{avg.}}(\mathcal{E}) &= \frac{1}{2} + \frac{1}{6}(\mathcal{E}_{22} + \mathcal{E}_{33} + \mathcal{E}_{44}) \\ &= \frac{1}{2} + \frac{1}{6}(p_0 + 2p_1) \end{aligned} \quad (12)$$

as in eqn. 7. Using eqn. 11, the effective channel  $\mathcal{C}$  from eqn. 9 can readily be expressed as

$$\mathcal{C} = \mathcal{E} \cdot \begin{pmatrix} 1 & 0 & 0 & 0 \\ 0 & (-1)^{b_2} p_1^m & 0 & 0 \\ 0 & 0 & (-1)^{b_1 + b_2} p_1^m & 0 \\ 0 & 0 & 0 & (-1)^{b_1} p_0^m \end{pmatrix}. \quad (13)$$

Therefore the survival probability is

$$\begin{aligned} \Pr(m, b_1, b_2) &= \text{Tr}(E \mathcal{C}(\rho)) \\ &= (-1)^{b_1} A p_0^m + ((-1)^{b_1 + b_2} B_1 + (-1)^{b_2} B_2) p_1^m + C, \end{aligned} \quad (14)$$

where

$$A := 2^{-1} \cdot \text{Tr}(E \cdot \mathcal{E}(Z)) \cdot \text{Tr}(\rho Z), \quad (15)$$

$$B_1 := 2^{-1} \cdot \text{Tr}(E \cdot \mathcal{E}(Y)) \cdot \text{Tr}(\rho Y), \quad (16)$$

$$B_2 := 2^{-1} \cdot \text{Tr}(E \cdot \mathcal{E}(X)) \cdot \text{Tr}(\rho X), \quad (17)$$

$$C := 2^{-1} \cdot \text{Tr}(E \cdot \mathcal{E}(\mathbb{I})). \quad (18)$$

Eqns. 4–6 then follow from appropriate choices of  $b_1, b_2$  and simple algebra.

*Characterizing the  $T$  gate.*—The  $T$  gate, or the  $R_8(1)$  operation (see eqn. 3), is important in many implementations since it is used to supplement the Clifford gates to achieve universal quantum computation. In leading approaches to fault-tolerant error-correction, the  $T$  gate is physically realized via magic-state injection [12], in which magic states are acted upon by Clifford transformation and post-selected stabilizer measurements. Because the physical (logical) Clifford gates are applied directly (transversally) whereas the  $T$  gate is implemented through the above method, the error on the  $T$  gate may be substantially different and requires separate characterization. While the quality of the injected gate can be assessed by measuring the quality of the input and output magic states as well as benchmarking the required stabilizer operations, here we provide a direct method to estimate the average gate fidelity of the  $T$  gate.

The  $T$  gate is contained in  $\mathcal{D}_8$  (see eqn. 2).  $\mathcal{D}_8$  can be divided in two cosets:  $\mathcal{D}_4$  and  $T \cdot \mathcal{D}_4$ .  $\mathcal{D}_4$ , a subgroup of  $\mathcal{D}_8$ , is generated by  $X$  and the phase gate  $S$ , which are both Clifford operations. If the average fidelity over  $\mathcal{D}_8$  and  $\mathcal{D}_4$  are similar, this is an indication that the  $T$  gate has similar average fidelity as the Clifford group. However, typically this will not hold for the reasons stated above, in which case we suggest the following protocol. First benchmark  $\mathcal{D}_4$  as per the above protocol. Then adapt interleaved randomized benchmarking [20] to the above protocol by replacing steps 3 and 4 (with  $j = 4$ ) with the two following steps:

3'. At each time step  $t = 1, \dots, m$ , apply  $R_8(1) \circ R_4(z_t)X^{x_t}$ .

4'. Apply the inversion gate, defined as

$$G_{\text{inv.}} := X^{b_1} Z^{b_2} \prod_{t=1}^m [R_8(1)R_4(z_t)X^{x_t}]^\dagger.$$

We require the sequence length to be even, so that the inversion gate is in  $\mathcal{D}_4$ . Fitting the two decay curves obtained from eqns. 5 and 6 allows the average fidelity  $\mathcal{F}_{\text{avg.}}(\mathcal{E}_T \circ \mathcal{E})$  of the composite noise map to be estimated via eqn. 7. The average fidelity of the  $T$  gate,  $\mathcal{F}_{\text{avg.}}(\mathcal{E}_T)$ , is then estimated from the approximation  $\chi_{00}^{\mathcal{E}_T \circ \mathcal{E}} = \chi_{00}^{\mathcal{E}} \chi_{00}^{\mathcal{E}_T}$  which is valid to within the implicit bound derived in [22]:

$$\begin{aligned} |\chi_{00}^{\mathcal{E}_T \circ \mathcal{E}} - \chi_{00}^{\mathcal{E}} \chi_{00}^{\mathcal{E}_T}| &\leq 2\sqrt{(1 - \chi_{00}^{\mathcal{E}})\chi_{00}^{\mathcal{E}}(1 - \chi_{00}^{\mathcal{E}_T})\chi_{00}^{\mathcal{E}_T}} \\ &\quad + (1 - \chi_{00}^{\mathcal{E}})(1 - \chi_{00}^{\mathcal{E}_T}), \end{aligned} \quad (19)$$

where in the qubit case

$$\chi_{00}^{\mathcal{E}} = \frac{3}{2} \mathcal{F}_{\text{avg.}}(\mathcal{E}) - \frac{1}{2}. \quad (20)$$

This bound is loose in general but tight when the Clifford gates in  $\mathcal{D}_4$  have much higher fidelity than the  $T$  gate (which is the regime of interest when optimizing the

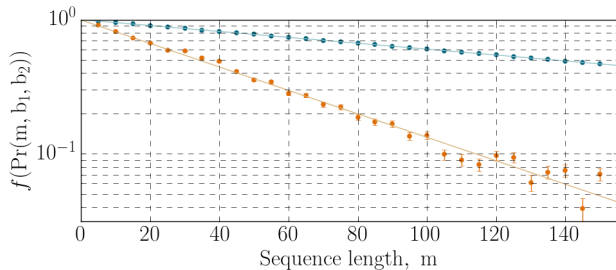


FIG. 2. (Color online) Decay curves corresponding to eqns. 5 and 6 for a standard randomized benchmarking simulation with  $A = \frac{1}{4}$  and  $B = \frac{1}{2}$  respectively. The shallow (blue) and steep (orange) lines correspond to eqn. 5 and eqn. 6 respectively. Each data point is obtained after averaging 500 sequences of fixed length. The noise model used to obtain this figure is described in the *Numerical simulation* section. Fits to the data give an estimated value for average fidelity over  $\mathcal{D}_8$  of 0.99257(9), which compares well with the true value of 0.9925.

overhead and fidelity of the distillation and injection routines) [23].

*Numerical simulation.*—Although the previous analysis is derived for gate- and time-independent noise, the randomized benchmarking protocol is both theoretically and practically robust to some level of gate-dependent noise [7, 19]. We now illustrate through numerical simulations that this robustness holds for the dihedral benchmarking protocol, particularly in the regime where the noise is strongly gate-dependent (as expected when the gates are implemented using different methods, namely, direct unitaries and magic state injection).

For our simulations, each operation within the dihedral group  $\mathcal{D}_8$  is generated by composing two gates; the first gate is in the subgroup generated by  $X$  and the phase gate  $S = R_8(2)$ , while the second gate is either identity or the  $T = R_8(1)$  gate. The error associated with the first gate is a simple depolarizing channel with an average fidelity of 0.9975. For the second gate, the error arises only after the  $T$  gate, and corresponds to an over-rotation with an average fidelity of 0.99. The total average fidelity over  $\mathcal{D}_8$  is 0.9925. Fig. 2 shows the two decay curves described by eqns. 5 and 6. Appropriate fits lead to a precise estimate of 0.99257(9) for the average fidelity.

We also simulate the interleaved randomized benchmarking protocol in two different regimes (see fig. 3). The first regime (fig. 3a) corresponds to over-rotation errors that are small for the Clifford operations, with average fidelity  $1 - 10^{-6}$ , but large for the  $T$  gate, with average fidelity  $1 - 10^{-2}$ . The estimate of the fidelity of the  $T$  gate via our protocol is extremely precise in this regime: 0.9902(3). The second regime (fig. 3b) corresponds to a similar over-rotation with average fidelity 0.99 both for the Clifford group and the  $T$  gate. In this case the estimated value of  $\mathcal{F}_{\text{avg.}}(\mathcal{E}_T)$  is 0.966 and the implicit bound from eqn. 19 only guarantees  $\mathcal{F}_{\text{avg.}}(\mathcal{E}_T)$  to lie the interval

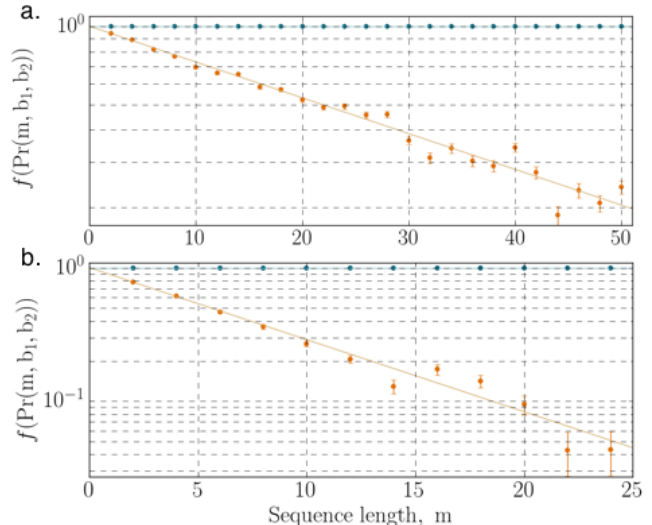


FIG. 3. Decay curves corresponding to eqns. 5 and 6 for an interleaved randomized benchmarking simulation with  $A = \frac{1}{4}$  and  $B = \frac{1}{2}$  respectively. The shallow (blue) and steep (orange) lines correspond to eqn. 5 and eqn. 6 respectively. Each data point is obtained after averaging 500 sequences of fixed length. The noise model used to obtain this figure is described in the *Numerical simulation* section. The top figure corresponds to high fidelity Clifford operations and a relatively noisy  $T$  gate. The bottom figure corresponds to errors of the same magnitude on the Clifford operations and the  $T$  gate. See text for details.

[0.928, 0.995]. The rather loose bound in this regime is an open problem for interleaved randomized benchmarking and is not specific to the current protocol.

*Conclusions.*—We have provided a protocol that extracts the average fidelity of the error arising over a group of single-qubit operations corresponding to the dihedral group. Of particular importance are  $\mathcal{D}_8$  and  $\mathcal{D}_4$ , which enable efficient and precise benchmarking of the  $T$  gate that plays a unique and important role in leading proposals for fault-tolerant quantum computation.

While we have explicitly assumed that the rotation axis is the  $z$  axis, this is an arbitrary choice. Since any single-qubit unitary can be written as a rotation about some axis on the Bloch sphere, our protocol can be used to characterize any single-qubit gate.

The essence of this paper is to realize that the 2-design restriction originally imposed in randomized benchmarking is too strict. Indeed, randomized benchmarking can be applied to any group whose Liouville representation contains few inequivalent irreps. Unraveling the class of all such algebraic structures is an open problem, though interesting groups such as  $\langle CZ, X, R_j(1) \rangle$  abound, which would allow gates such as the  $T$  gate to be characterized ‘in vivo’ within an  $n$ -qubit circuit [24].

*Acknowledgments*— This research was supported by the U.S. Army Research Office through grant W911NF-14-1-0103, CIFAR, the Government of Ontario, and the

- 
- [1] I. L. Chuang and M. A. Nielsen, *Journal of Modern Optics* **44**, 2455 (1997).
- [2] J. F. Poyatos, J. I. Cirac, and P. Zoller, *Physical Review Letters* **78**, 390 (1997).
- [3] S. T. Merkel, J. M. Gambetta, J. A. Smolin, S. Poletto, A. D. Córcoles, B. R. Johnson, C. A. Ryan, and M. Steffen, *Physical Review A* **87**, 062119 (2013).
- [4] J. Emerson, R. Alicki, and K. Życzkowski, *Journal of Optics B: Quantum and Semiclassical Optics* **7**, S347 (2005), arXiv:0503243 [quant-ph].
- [5] E. Knill, D. Leibfried, R. Reichle, J. Britton, R. B. Blakestad, J. D. Jost, C. Langer, R. Ozeri, S. Seidelin, and D. J. Wineland, *Physical Review A* **77**, 012307 (2008).
- [6] E. Magesan, J. M. Gambetta, and J. Emerson, *Physical Review Letters* **106**, 180504 (2011).
- [7] E. Magesan, J. M. Gambetta, and J. Emerson, *Physical Review A* **85**, 042311 (2012).
- [8] C. Dankert, R. Cleve, J. Emerson, and E. Livine, (2006), arXiv:0606161v1.
- [9] C. Dankert, R. Cleve, J. Emerson, and E. Livine, *Physical Review A* **80**, 012304 (2009).
- [10] D. Gottesman, *Proceedings of Symposia in Applied Mathematics* **68**, 13 (2010), arXiv:0904.2557v1.
- [11] Y. R. Sanders, J. J. Wallman, and B. C. Sanders, (2015), arXiv:1501.04932.
- [12] S. Bravyi and A. Kitaev, *Physical Review A* **71**, 022316 (2005), arXiv:0403025v2 [arXiv:quant-ph].
- [13] A. M. Meier, B. Eastin, and E. Knill, (2012), arXiv:1204.4221.
- [14] E. Magesan, J. M. Gambetta, B. R. Johnson, C. A. Ryan, J. M. Chow, S. T. Merkel, M. P. da Silva, G. A. Keefe, M. B. Rothwell, T. A. Ohki, M. B. Ketchen, and M. Steffen, *Physical Review Letters* **109**, 080505 (2012), arXiv:1203.4550.
- [15] A. J. Landahl and C. Cesare, (2013), arXiv:1302.3240.
- [16] S. Forest, D. Gosset, V. Kliuchnikov, and D. McKinnon, (2015), arXiv:1501.04944.
- [17] G. Duclos-Cianci and D. Poulin, *Physical Review A* **91**, 042315 (2015), arXiv:1403.5280.
- [18] C. Granade, C. Ferrie, and D. G. Cory, *New Journal of Physics* **17**, 1 (2014), arXiv:arXiv:1404.5275v1.
- [19] J. J. Wallman and S. T. Flammia, *New Journal of Physics* **16**, 103032 (2014), arXiv:1404.6025.
- [20] J. M. Gambetta, A. D. Córcoles, S. T. Merkel, B. R. Johnson, J. a. Smolin, J. M. Chow, C. a. Ryan, C. Rigetti, S. Poletto, T. a. Ohki, M. B. Ketchen, and M. Steffen, *Physical Review Letters* **109**, 240504 (2012), arXiv:arXiv:1204.6308v1.
- [21] M. A. Nielsen, *Physics Letters A* **303**, 249 (2002).
- [22] S. Kimmel, M. P. da Silva, C. A. Ryan, B. R. Johnson, and T. Ohki, *Physical Review X* **4**, 011050 (2014), arXiv:1306.2348.
- [23] A. G. Fowler, M. Mariantoni, J. M. Martinis, and A. N. Cleland, *Physical Review A* **86**, 032324 (2012), arXiv:1208.0928.
- [24] A. C. Dugas, J. Wallman, and J. Emerson, (2015), work in progress.